Journal of Oil Palm Research
DOI: https://doi.org/10.21894/jopr.2023.0054

PALM KERNEL MEAL ACTIVATED CARBON VIA GLASS WOOL-PYROLYSIS METHOD FOR CEFTRIAXONE ADSORPTION

ACHMAD GUS FAHMI[1]; ZAENAL ABIDIN[2]*; CECEP KUSMANA[3] and ERLIZA NOOR[4]

ABSTRACT

Antibiotic residues are a primary environmental concern because they are difficult to remove, including in wastewater treatment plants. A one-pot glass wool-pyrolysis method was developed and utilised to convert palm kernel meal into activated carbon from palm kernel meal (AC-PKM) over process temperatures 750°C for 5 hr as an adsorbent for antibiotic residues. Physicochemical properties, semi-quantitative specific surface area, surface functional group profiles, and scanning electron microscopy (SEM) were evaluated. The physicochemical properties of AC-PKM meet the standards set by SNI 06-3730-1995 with a semi-quantitative specific surface area of 751 m^2/g. Fourier transform infrared (FTIR) analysis shows that the active functional groups are scattered on the surface of AC-PKM. The maximum adsorption capacity is 82.64 mg/g adsorbent and can be explained by the Langmuir isotherm and pseudo-second-order type I kinetic model. The thermodynamic investigation showed that the adsorption process is a spontaneous endothermic reaction. The AC-PKM can remove 26% ceftriaxone (as a model residue antibiotic) for 2 hr of contact at a neutral pH at room temperature. The results show great promise of the one-pot glass wool-pyrolysis method to produce desirable activated carbon for removing ceftriaxone (CFT) application and an alternative treatment for the reuse of palm kernel meal waste.

Keywords: adsorption, ceftriaxone, glass wool, palm kernel meal, pyrolysis.

Received: 21 July 2022; **Accepted:** 14 August 2023; **Published online:** 26 October 2023.

INTRODUCTION

Antibiotics are drugs used to treat bacterial infections. There is no doubt about the benefits of using antibiotics. However, if used excessively or not according to indications, it will lead to strains of bacteria resistant to antibiotics. Repeated and irrational use of the same antibiotic can increase microbial resistance to that antibiotic (Olesen *et al*., 2018). Its increasing use in COVID-19 pandemic and antimicrobial resistance is a severe threat to public health that is experienced globally (Browne *et al*., 2021). Previous studies have explained that excessive use of antibiotics can lead to other diseases, such as diabetes mellitus (Mensah and Ansah, 2016) and cancer (Prajwal *et al*., 2017). The results of research conducted by Widayati *et al*. (2011) showed that antibiotic abuse does not only occur in health facilities but also in the community. Antibiotics are also used in livestock and fisheries, so antibiotic residues are considered persistent micropollutants in the aquatic environment.

Among various antibiotics, ceftriaxone (CFT) is the most common group in production and use in Indonesia because it has antimicrobial activity against various bacterial pathogens (Ayele *et al*., 2018). However, the CFT residue will enter the hospital wastewater treatment plant, which

[1] Graduate School of Natural Resources and Environmental Management Science, IPB University, 16127 Bogor, Indonesia.

[2] Department of Chemistry, Faculty of Mathematics and Natural Science, IPB University, 16680 Bogor, Indonesia.

[3] Department of Silviculture, Faculty of Forest and Environment, IPB University, 16680 Bogor, Indonesia.

[4] Department of Agro-Industrial Engineering, Faculty of Agriculture Engineering, IPB University, 16680 Bogor, Indonesia.

* *Corresponding author e-mail: abidinzed@apps.ipb.ac.id*

harms the aquatic environment and can hinder the progress of water treatment processes that use microbes. In addition, irrational use can lead to increased resistance to microorganisms and become a significant public health crisis (Al-Riyami *et al*., 2018). Therefore, efforts are needed to remove CFT residues from water so they are not harmful to the environment.

In recent years, various techniques have been investigated for the removal of CFTs from wastewater, including photocatalytic treatment, oxidation degradation (Kordestani *et al*., 2020), ultrasonic wave degradation (Shi *et al*., 2020), adsorption (Mahmoud *et al*., 2020), bio-electrochemical degradation (Hassan *et al*., 2021) and biological treatment (Bozorginia *et al*., 2021). Among these techniques, adsorption has been considered one of the most prospective approaches in the future because of its attractive advantages for the application of drug waste management in wastewater (de Ilurdoz *et al*., 2022). Several alternative adsorbents to overcome this problem are kaolin, bentonite (Song *et al*., 2019), polymer resins (Rivas *et al*., 2020), metal-organic framework (MOF) (Zango *et al*., 2020) and activated carbon (Schultz *et al*., 2020).

Important factors that constrain the selection and use of adsorbents are raw material availability, adsorption effectiveness, manufacturing method and production price. The challenges for raw material availability are overcome by using alternative raw materials derived from waste or recycling. In contrast, adsorption effectiveness, manufacturing methods and production prices are overcome by modifying production methods to produce adsorbents that have large surface areas, are easy, simple, and do not require expensive costs in manufacturing. One of the most widely used adsorbents, activated carbon, is the best alternative that can be chosen. Activated carbon can be produced from waste and has sustainable and environmentally friendly properties (Sharma *et al*., 2020). This potential can be an opportunity for tropical countries such as Indonesia because it fulfils promising aspects for providing such activated carbon adsorbents. However, even poorly managed biomass can cause serious environmental problems.

As one of the most widely used adsorbents, activated carbon is also considered a reliable solution for CFT removal due to its good performance (Schultz *et al*., 2020). On the other hand, activated carbon from palm fibres have a good adsorption capacity (57.47 mg/g adsorbent) in removing antibiotic residues in water (Acelas *et al*., 2021). One of the palm oil wastes that can be converted into activated carbon is palm kernel meal (PKM). PKM is a solid by-product of palm kernel oil extraction. Oil palm biomass waste from empty fruit bunches, core meat, shells, and a mixture of them, has been widely used as activated carbon as an adsorbent of organic compounds (Ukanwa *et al*., 2020). Rugayah *et al*. (2014) used steam activation at high temperatures to make activated carbon from palm shells. This condition produces activated carbon with an adsorption capacity of 80.7% or 8.83 mg/g compared to commercial activated carbon. However, the continuous high-temperature steam method causes the production cost to increase. According to Osman *et al*. (2016), the one-step physical activation method can reduce production costs. The single-step physical activation method has a surface area of 523 m^2/g with an organic compound adsorption capacity of 13-38 mmol/g adsorbent (Fahmi *et al*., 2019). In addition, modification of glass wool in the process of making activated carbon has the benefit of increasing the percentage yield, reducing the amount of ash formed and providing activated carbon with surface functional groups maintained (Fahmi *et al*., 2022). However, applying activated carbon products from PKM with physical activation has not been widely used to remove antibiotic waste in water. Therefore, this study discusses the properties of AC-PKM by the one-pot glass wool pyrolysis method developed by Fahmi *et al*. (2019) and relevant factors for CFT removal in wastewater.

MATERIALS AND METHODS

Materials

Granule PKM waste was collected at a palm oil plant in South Kalimantan, Indonesia. All the chemicals used were obtained from Sigma-Aldrich®, while the commercially activated carbon used as control (ACC) was purchased from a chemical store in Bogor. The antibiotics model used in all the experiments was CFT, a sodium salt. The structure of CFT is given in *Figure 1*.

Procedures

Sample preparation. Waste PKM was collected from the oil palm industry in South Kalimantan. To remove contaminants, the sample was washed with distilled water before drying in the oven for 24 hr at 105°C. The dried materials were cut into small pieces and ground to 100 mesh using fibre grinder (Model 4 Wiley Mill Machine, Thomas Scientific USA) at 5000-6000 rpm. Synthesis of AC-PKM followed the modified method by Fahmi *et al*. (2019). 5 g of PKM powder was added in crucible porcelain-coated glass wool all around. Then the porcelain crucible was heated at 750°C in a *47900 Thermocline furnace* (Barnstead International, USA) for 5 hr. This process took 3 hr for carbonisation and 2 hr for physical activation with characteristics of activated carbon showed in Fahmi *et al.* (2022). It was then cooled naturally to room temperature.

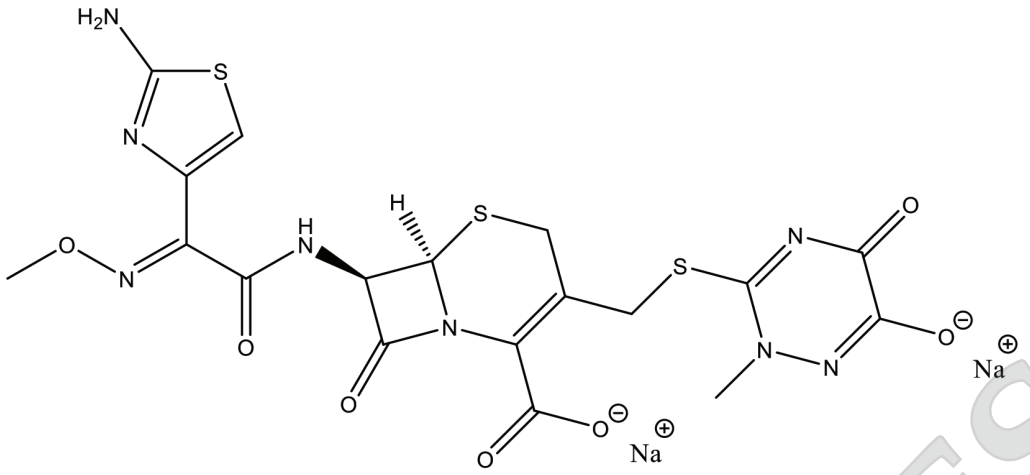

Figure 1. Structure of sodium ceftriaxone.

Characterisation of activated carbon. Physico-chemical properties of AC-PKM, PKM, and ACC (as a control), such as pH, ash content and moisture content, were determined using standard methods for activated carbon. The pH value of activated carbon was determined according to American Standard Testing Method (ASTM) D3838-5 with 1 g of sample added to 100 mL of distilled water in a 250 mL beaker. After stirring continuously for 10 min, the activated carbon was filtered, and the filtrate solution acidity was determined using a pH meter. The ash content of activated carbon was determined using the ASTM D2866-96 method. Moisture content was determined using the oven drying method as described in ASTM D2867-09. The specific surface area of activated carbon was calculated using semi-quantitative measurements (Okeola *et al*., 2012). Surface functional groups were identified using Spectrum One Fourier transform infrared (FTIR) (Perkin-Elmer, USA). The morphology of AC-PKM was identified using a scanning electron microscope (JEOL JSM-IT 300, Tokyo, Japan). All chemical ingredients were obtained from Sigma-Aldrich®.

Adsorption of CFT. CFT was employed as an antibiotic model because this drug is often used in hospital therapy. In evaluating the stability of CFT under acidic, alkaline, and heat conditions, the CFT solution (25 mg/L) was treated with acid at pH 1, alkaline at pH 13, and temperature at 40°C (313 K). After being stored for 24 hr, the CFT solution was scanned using a Genesys 10S Ultraviolet visible (UV-Vis) spectrophotometer (Thermo Fischer Scientific, USA) at 200-400 nm wavelength to identify degradation or peak shift. Adsorption was carried out at pH neutral with the batch method for 24 hr at 25°C (298 K). A total of 10 mL of CFT solution with a concentration of 25-1000 mg/L was added to a tube containing AC-PKM sample as much as 0.01 g. After equilibrium, the adsorbent was separated under centrifugation, and the concentration of CFT on the supernatant was measured using Genesys 10S UV-Vis spectrophotometer (Thermo Fischer Scientific, USA) at the maximum wavelength (274 nm). The adsorption capacity followed Equation (1):

$$q_e = \frac{(C_o\text{-}C_e)\ x\ V}{(m\ x\ 1000)}. \quad (1)$$

where q_e is adsorption capacity (mg/g adsorbent), V is the volume of solution (mL), C_o is the initial concentration of CFT (mg/L), C_e is the residual concentration of CFT (mg/L), and m is mass of adsorbent (g). Mathematical representation from the isotherm adsorption model was used to interpret CFT adsorption on the surface adsorbent, and its calculation refers to Langmuir and Freundlich isotherm model. The Langmuir isotherm model in its nonlinear form is expressed as in Equation (2) (Jasper *et al.*, 2020).

$$q_e = \frac{q_{max} K_L C_e}{1 + K_L C_e} \quad (2)$$

where, q_e being adsorption capacity equilibrium of the adsorbent (mg/g adsorbent), C_e being the residual concentration (mg/L), q_{max} being adsorption maximum in Langmuir model (mg/g adsorbent), being Langmuir's constant (L/mg) that represents affinity side active bond. The Freundlich isotherm model in nonlinear form is expressed as in Equation (3) (Jasper *et al.*, 2020).

$$q_e = K_f C^{\frac{1}{n}} \quad (3)$$

where, q_e as adsorption capacity equilibrium (mg/g adsorbent), C_e is the residual concentration (mg/L), K_f (mg/g) (L/mg)$^{(1/n)}$, and $1/n$ is Freundlich constant denoting capacity adsorption and intensity adsorption. The process was solely based on C_e

measurements. Following the statistical premise, Cassol *et al*. (2014) state that the method is more trustworthy and must be used to estimate the adsorption equilibrium parameters.

Kinetic and thermodynamic models. The method for analysing the adsorption kinetics was carried out with the same experiment as the adsorption measurement. The treatment was repeated by measuring the supernatant at different contact times (0-180 min). In addition, the effect of temperature on the adsorption process of CFT on AC-PKM was studied by varying the adsorption temperature at 30°C (303 K) until 40°C (313 K).

Removal of CFT. CFT removal was carried out at a CFT concentration of 250 mg/L as artificial wastes. The quantity of CFT removal (%R) by AC-PKM was calculated as follows [Equation (4)].

$$\%R = \frac{V\,(C_O - C_e)}{C_O} \times 100 \quad (4)$$

where $\%R$ is percentage removal CFT (%), V is volume of solution (mL), C_o is initial concentration of CFT (mg/L), and C_e is the residual concentration of CFT (mg/L).

RESULTS AND DISCUSSION

Adsorbent Characteristics

Generally, activated carbon is synthesized at temperatures of 700°C-1000°C. In high-temperature condition, some of the carbon loses various functional groups on its surface and convert to ash. The presence of this surface functional group is significant because it plays a role in chemical processes for adsorption and catalysis. Xiao *et al*. (2018) used a unique pyrolysis process to retain functional groups on the surface, and this method can increase specific surface area, porosity, and absorptivity. Thus, maintaining functional groups on the surface of activated carbon has benefits in utilising the activated carbon.

This study concentrated on the physical activation approach using glass wool as a material that can isolate heat and reduce oxygen during the activation process. Furthermore, adding glass wool to coat the reactor can cause the heat generated to be concentrated in the reactor core, making the pyrolysis process more efficient (Santhiarsa, 2021). Our previous experiment used the glass wool pyrolysis method for coconut shell waste samples, effectively conducted at 750°C to produce activated carbon with large surface functional groups. This method can also increase biomass conversion into activated carbon (Fahmi *et al*., 2019). In addition, the modification of glass wool in the process of making activated carbon has the benefit of increasing the percentage yield, reducing the amount of ash formed, and providing activated carbon with surface functional groups maintained (Fahmi *et al*., 2022). Therefore, in this study, we used the similar method with different biomass effluents to apply ceftriaxone removal in hospital wastewater.

The physicochemical properties of the activated carbon are presented in *Table 1*. Based on the measurement results, it is shown that the pH values of AC-PKM and ACC were found to be in proximity of neutral pH, namely 6.80 and 6.98, respectively. Generally, the acceptable pH range is 6.00-8.00 for applications in wastewater treatment (Ashtaputrey and Ashtaputrey, 2016). The presence of surface-active functional groups can affect the surface charge of the adsorbent (variable charge), which will affect the adsorption ability. Therefore, the pH value is crucial for adsorbents with surface-active functional groups to achieve the most excellent application performance.

TABLE 1 . PHYSICOCHEMICAL PROPERTIES OF AC-PKM COMPARED WITH COMMERCIAL ACTIVATED CARBON (ACC) AND BIOMASS (PKM)

Parameter	AC-PKM	ACC	PKM
pH	6.80 ± 0.2	6.98 ± 0.2	-
Ash content (%)	5.10 ± 1.0	3.10 ± 1.0	5.15 ± 1.0
Moisture content (%)	4.94 ± 1.0	3.94 ± 1.0	14.94 ± 1.0
Specific surface area (m^2/g)	751 ± 10	783 ± 10	407 ± 10

Another physicochemical property is ash content. Based on the measurement, the ash content of AC-PKM and PKM had the same values, which were 5.10% and 5.15%, respectively, while ACC has a lower ash content value of 3.10%. Ash content can affect the activated carbon quality, with the maximum in activated carbon being 15.00% (SNI 06-3730-1995). High ash content can reduce the absorption and specific surface area (De Gisi *et al*., 2016). In addition, the selection of biomass raw materials also affects the ash content in activated carbon. Low ash-content biomass has the potential as an excellent raw material for the manufacture of activated carbon (Feng *et al*., 2020).

Furthermore, AC-PKM has a relatively low water moisture of 4.94%, with the accepted standard value for activated carbon samples of 3.00%-6.00% (Gumus and Okpeku, 2015). In addition, the high water moisture in activated carbon will dilute the adsorbent concentration, thus requiring more weight of the adsorbent to maintain the same adsorption capacity. Furthermore, the water moisture decreases with the carbonisation temperature due to the

smaller pores of the activated carbon. The high water moisture is usually caused by the concentration of activator in chemical activation (Maulina *et al*., 2020). Ultimately, this phenomenon will increase the hygroscopic properties of absorbing water from the air (Tani *et al*., 2014). Hence, the selection of activator compounds and activation methods have an essential role in influencing the characteristics of the water moisture in activated carbon.

Based on the written reports, the value of X_m was used to calculate the specific surface area of monolayer coverage (Okeola *et al*., 2012). The specific surface area of AC-PKM is 751 m^2/g, slightly lower than that of ACC (783 m^2/g). According to Hu and Gao (2018), a high surface area can increase the adsorbability so that it will affect the adsorption capacity of the adsorbent. In addition, another factor that affects the adsorption ability is the surface interaction of the adsorbent with the adsorbate, which is predicted through the adsorption isotherm model (Wu *et al*., 2020). Activated carbon has various pores, so further analysis is needed to show the presence of macropores, mesopores and micropores.

In addition, the adsorption performance of carbon-based adsorbents is highly dependent on the surface-active functional groups (Kharrazi *et al*., 2021). In this study, the various surface-active functional groups of AC-PKM, ACC, and PKM was identified using FTIR spectroscopy (*Figure 2*). The AC-PKM and PKM show a broad spectrum around 3445 cm^{-1} and 600 cm^{-1} with different intensities and shapes of the spectra. Meanwhile, the ACC found that the peak loss was at the wavenumber at 3445 cm^{-1}, which is a stretch of O-H and 600 cm^{-1} from the =C-H bending of the aromatic ring. Another FTIR spectrum of ACC differed in intensity from the spectrum of AC-PKM and PKM. The C=O (1500-1650 cm^{-1}) and C-O (1000-1050 cm^{-1}) stretches had low intensity in the spectrum of ACC, and the CC (2366 cm^{-1}) stretch band was weak. However, the similarity of the spectrum of AC-PKM with the initial biomass (PKM) is identical, which indicates that there are similar functional groups. Thus, the glass wool-pyrolysis method can maintain the intensity of the spectrum compared to ACC, where the spectrum is significantly weakened or even disappears.

Based on the spectrum data analysed for each adsorbent produced, it can be seen that AC-PKM has a peak in the FTIR spectrum in the form of some active surface groups. Therefore, the morphology of AC-PKM was confirmed using Scanning Electron Microscope (SEM). The identification results using SEM showed that on the surface of the AC-PKM pore, there was an unshaped bulk solid. In addition, these unshaped bulk solids can also reduce the pore size but provide interaction with the adsorbate adsorbed. As for ACC, there are no such shapeless bulk solids, which corroborates the statement of the presence of functional groups on the AC-PKM pore surface (*Figure 3*).

CFT stability experiments showed that CFT has high stability in heat treatment because there was no significant change (24 hr, 40°C) (*Figure 4*). Roca *et al*. (2011) suggest that β-lactam antibiotics such as CFT will undergo thermal decomposition gradually at a temperature of 60°C-100°C following pseudo-first-order kinetics. Meanwhile, at room temperature (23 ± 2°C), structurally, CFT is very stable for up to 4 days (De Diego *et al*., 2010). However, in the acid-base treatment, there were (hyperchromic and bathochromic) shifts in the peak of the CFT, which indicated that it was unstable (*Figure 4*). This condition is caused by the side reactions, such as hydrolysis, and side functional groups, such as

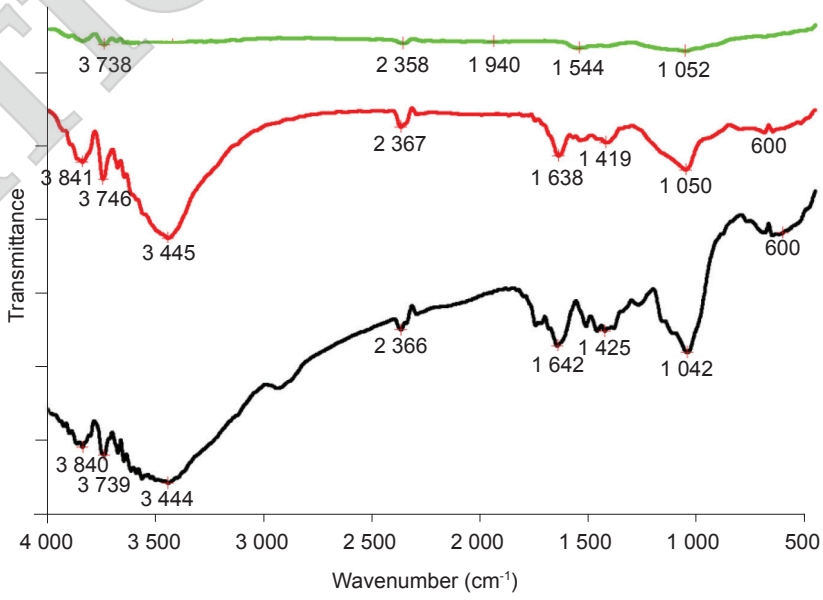

Figure 2. The infrared spectrum of ACC (green line), AC-PKM (red line) and PKM (black line).

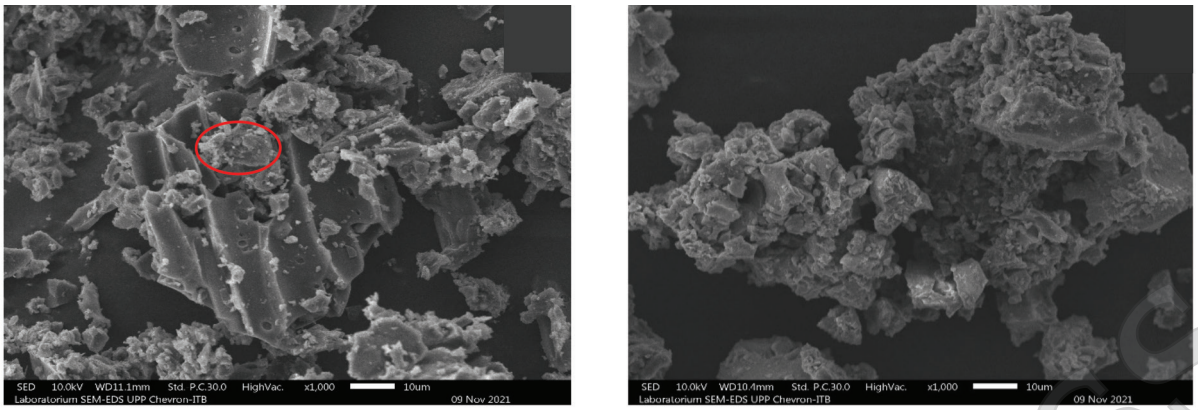

Figure 3. Scanning electron microscope photograph of (a) AC-PKM, and (b) ACC.

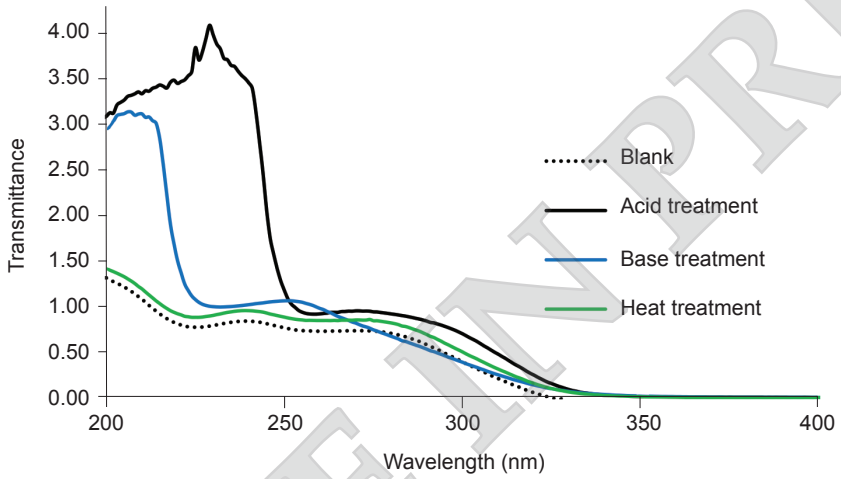

Figure 4. UV spectrum of CFT in 200-400 nm with various treatments (acid, base and heat).

amines and carboxyls, that affect the structural changes of CFT (Alekseev, 2010). Based on these results, adsorption measurements were carried out under neutral conditions according to the pH of the activated carbon and CFT.

CFT Adsorption

Sorption processes are well described by isotherms whose purpose is to help elucidate the interaction between sorbate and sorbent. They also provide information on the affinity of the sorbent for the sorbate. In this study, the Langmuir and Freundlich isotherm models were applied to observe the sorption of CFT onto the AC-PKM. All three adsorbents (ACC, AC-PKM and PKM) followed the Langmuir adsorption isotherm, consistent with the statistical premise with non-linear evaluation (*Figure 5*).

The isotherm models shown in *Table 2* follow the Langmuir model for all three adsorbent types ACC, AC-PKM, and PKM. The linearity (R^2) of the Langmuir adsorption isotherm model for ACC, AC-PKM, and PKM significantly differed from the linearity (R^2) of the Freundlich adsorption isotherm model. According to Cassol *et al*. (2014), this method is more reliable and should be used to determine adsorption equilibrium parameters. This isotherm model is routinely used to explore the adsorption characteristics of an adsorbent (Karri *et al*., 2017). As for the two adsorption isotherm models, they have differences from the adsorption mechanism that occurs with various assumptions in each model. The Freundlich isotherm model predicts sites that do not interact with heterogeneous surfaces and exponential adsorption. In contrast, the Langmuir model predicts sites that interact with the heterogeneous surface and exponential adsorption.

TABLE 2. LANGMUIR AND FREUNDLICH ADSORPTION ISOTHERM MODEL CONSTANTS

Adsorbent	Langmuir			Freundlich		
	qm	b	R^2	Kf	n	R^2
PKM	24.86	0.033	0.9891	20.19	44.05	0.1572
AC-PKM	82.64	0.037	0.9982	14.56	3.71	0.9162
ACC	153.85	0.029	0.9988	16.64	2.75	0.9091

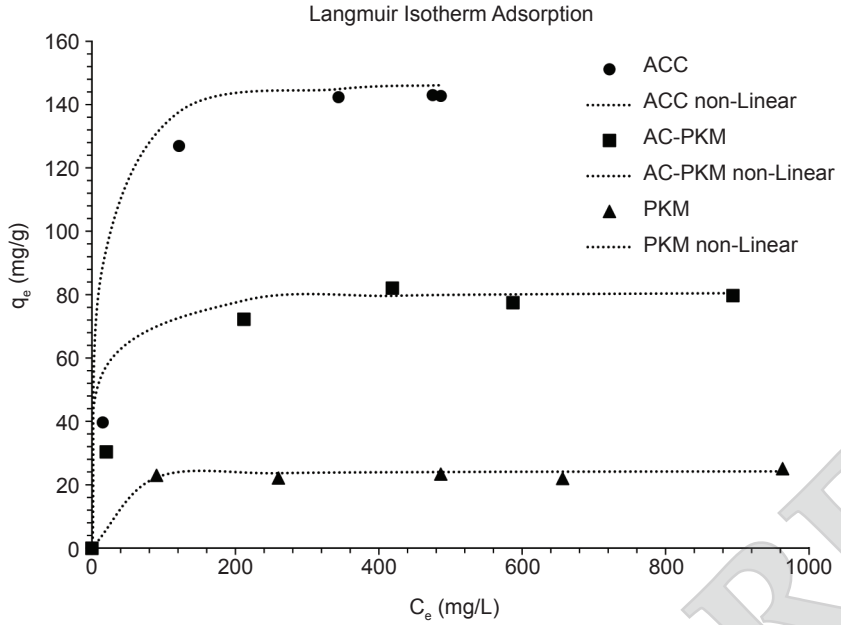

Figure 5. Nonlinear the Langmuir isotherm model fittings for CFT adsorption onto ACC, AC-PKM and PKM at room temperature.

The maximum adsorption capacity of each sample was determined by calculating the Langmuir adsorption isotherm (*Figure 5*). The maximum adsorption capacity value of PKM is 24.86 mg/g adsorbent was the lowest when compared to AC-PKM (82.64 mg/g adsorbent), and ACC (153.85 mg/g adsorbent). The activated carbon adsorption mechanism generally utilises wide pores or follows the Freundlich adsorption isotherm model (Ayawei *et al*., 2017). However, the presence of surface functional groups can affect the adsorption capacity. CFT adsorption in water was carried out at neutral pH, so the anionic CFTs dominated. However, the negatively charged surface of AC-PKM electrostatically repels the incoming CFT anions and affects their absorption. Furthermore, competition of hydroxyl (-OH) functional groups for the active binding site on AC-PKM with CFT anions may contribute to the markedly perceived decrease in adsorption rates (Saied *et al*., 2022). Therefore, the adsorption capacity will decrease as the surface functional groups increase. The maximum monolayer adsorption capacity (q_{max}) was 82.64 mg/g adsorbent, comparable to values reported for CFT adsorption with several adsorbents (*Table 3*).

The dependence of pH on CFT stability (*Figure 4*) implies that the removal of CFTs under neutral conditions cannot be ascribed to electrostatic interactions. This is because the CFT used as a drug is a sodium salt compound easily soluble in water with a pH of around 6.7 (Khan *et al*., 2017). In addition, the crystal structure of CFT has many OH---O hydrogen bonds involving water molecules and an ionised portion of the anion (Gonzalez *et al*., 2020), so it will produce a high electrostatic repulsion force with the surface-active group of activated carbon, which is also negatively charged. The electrostatic repulsion between AC-PKM and CFT can reduce the adsorption capacity of AC-PKM compared to commercial activated carbon (ACC).

TABLE 3. COMPARISON OF MAXIMUM ADSORPTION CAPACITY OF CFT USING SAVERAL ADSORBENTS

Adsorbent	q_{max} (mg/g adsorbent)	References
Activated carbon-Fe_2O_3	28.930	Badi *et al.* (2018)
ZVI/$SrFe_{12}O_{19}$	8.084	Amiri *et al.* (2020)
NBent-$NTiO_2$-Chit nanocomposite	90.910	Mahmoud *et al.* (2020)
Bi_2WO_6/g-C_3N_4 photocatalyst	3.400	Zhao *et al.* (2018)
ACC	153.850	Present study
AC-PKM	82.640	Present study

The interactions that may form so AC-PKM can adsorb CFT are non-electrostatic interactions such as H-bonds, -π interactions, n-π electron donor-acceptor interactions, and hydrophobic-hydrophobic interactions (Saied *et al*., 2022). Although there is a possible interaction between CFTs with π-π bonds in the activated carbon pores (*Figure 6*). Hydrogen bonds occur between the hydroxyl functional groups on the activated carbon surface and *S*, *N*, and *O* atoms in the CFT structure (C-OH---S, C-OH---N, and C-OH---O). Gonzales *et al*. (2020) report that hydroxyl molecules act as donors for ionised carboxylates and carbonyls. In addition, there are also intramolecular hydrogen

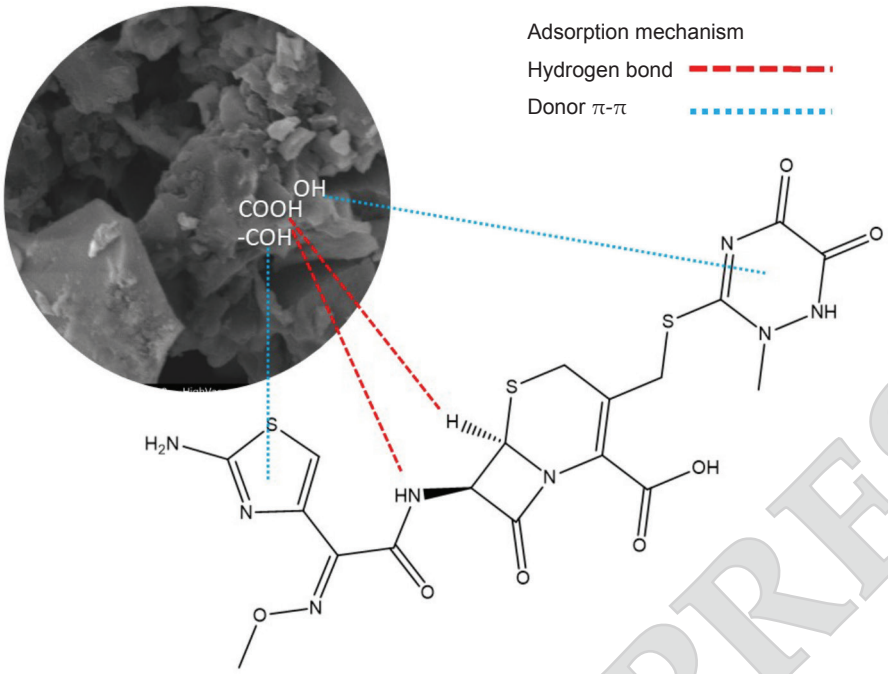

Figure 6. Proposed adsorption mechanism of ceftriaxone as a model antibiotics residue in this study to activated carbon from PKM.

bonds C13-H48-C10 with the carbon of the ionised carboxyl group. Another interaction that may occur in this adsorption process is between the carbonyls found on the activated carbon surface and triazine (aromatic) in the CFT structure. The *n*-π electron donor-acceptor interaction occurs when the carbonyl donates a lone pair of electrons (*n*), and the triazine accepts electrons in its system structure. According to Biasutti *et al*. (1992), nitrogen-substituted benzene, such as triazine, is an acceptor in the *n*-π electron donor-acceptor interaction. Therefore, the adsorption mechanism can be illustrated in *Figure 6*.

Kinetics and Thermodynamics Model of CFT Adsorption

Experiments to obtain CFT removal percentage were carried out at room temperature and neutral pH using an artificial CFT waste (250 mg/L). Gradually, the concentration of CFT in the residual solution was measured to obtain a stable condition at several points (*Figure 7*). Based on the measurements, the results showed that PKM could absorb the lowest value of 8%. The AC-PKM conversion using the glass wool-pyrolysis method can increase the percentage of CFT removal is to 26%. However, this value is still lower when compared to ACC (32%). This percentage value has been able to eliminate the content of CFT in hospital wastewater with a concentration of 1.25-29.15 g/mL (Shipingana *et al.*, 2022).

Adsorption is also a multistep process involving the transfer of dissolved substances to the surface, followed by diffusion of internal pores. Thus, kinetics adsorption gives valuable information for the design need of big-scale adsorption columns. There are two types of kinetic study models, *i.e.*, pseudo-first-order model and pseudo-second-order model. The pseudo-first-order assumes that the interaction surface controls the adsorption process. In contrast, pseudo-second-order assumes that intra-particle diffusion controls the adsorption rate. Lagergren first proposed this kinetic study model to describe the adsorption of pollutant liquid on the surface solid and differentiate it from the kinetic system based on concentration (Vafakhah *et al*., 2016). The experimental results of the kinetic parameters are given in *Table 4* and *Figure 8*. The linear correlation coefficient of AC-PKM (R^2) against the pseudo-second-order kinetic model type I (R^2=0.9961) was higher than that of the other kinetic model. In addition, the experimental adsorption capacity value on pseudo-second-order kinetics model type I (q_{exp}=82.64 mg/g) was close to the calculated one (q_{cal}=72.9927 mg/g), indicating this kinetic model is more suitable for describing the data. Therefore, the phenomenon of CFT adsorption with AC-PKM is chemisorption (Yu *et al*., 2020).

Thermodynamic analysis was also carried out to predict changes in free energy ($G°$), enthalpy ($H°$), and entropy ($S°$) (Bhandari and Gogate, 2018). The adsorption usually involves dropping Gibbs free energy (ΔG), accompanied by decreased entropy (ΔS), because the adsorbed molecule is bound to the side of the active surface. The loss of degrees of freedom of adsorbed molecules compared with the state before adsorption causes a drop in free energy (ΔG) and entropy (ΔS). At the same time, enthalpy (ΔH) depends on temperature during adsorption. Temperature plays a vital role in adsorption. Change

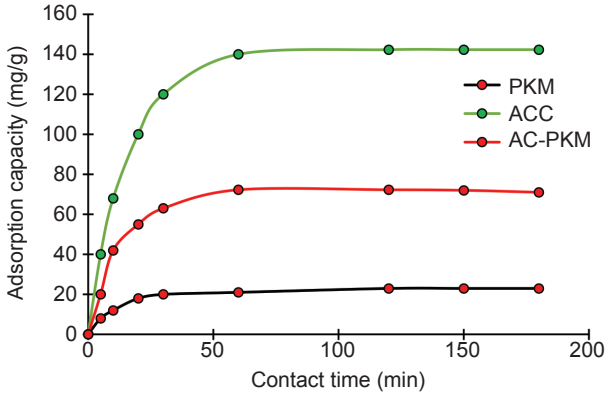

Figure 7. Adsorption capacity of CFT removal (mg/g adsorbent) with the effect of contact time on ACC, AC-PKM and PKM biomass.

TABLE 4. ADSORPTION KINETICS CONSTANTS OF PSEUDO-FIRST-ORDER AND PSEUDO-SECOND-ORDER ADSORPTION

Type	Non-linear form	Linear form	Plot	Parameters
Pseudo first-order	$q = q_e(1 - exp^{-K_1 t})$	$\log(q_e - q) = \log(q_e) - \frac{K_1 t}{2.303}$	$\log(q_e - q)$ vs. t	$K_1 = -2.303$ x slope
Type 1 pseudo second-order		$\frac{t}{q} = \frac{1}{K_2 q_e^2} + \frac{1}{q_e} t$	t/q vs. t	$q_e = 1/\text{slope}, K_2 = \text{slope}^2/\text{intercept}$
Type 2 pseudo second-order		$\frac{1}{q} = \left(\frac{1}{K_2 q_e^2}\right)\frac{1}{t} + \frac{1}{q_e}$	$1/q$ vs. $1/t$	$q_e = 1/\text{intercept}, K_2 = \text{intercept}^2/\text{slope}$
Type 3 pseudo second-order	$q = \frac{K_2 q_e^2 t}{1 + K_2 q_e t}$	$\frac{1}{t} = \frac{K_2 q_e^2}{q} - \frac{K_2 q_e^2}{q_e}$	$1/t$ vs. $1/q$	$q_e = -\text{slope}/\text{intercept}, K_2 = \text{intercept}^2/\text{slope}$
Type 4 pseudo second-order		$\frac{q}{t} = K_2 q_e^2 - \frac{K_2 q_e^2 q}{q_e}$	q/t vs. q	$q_e = -\text{intercept}/\text{slope}, K_2 = \text{slope}^2/\text{intercept}$
Type 5 pseudo second-order		$\frac{1}{q_e - q} = \frac{1}{q_e} + K_2 t$	$1/(q_e - q)$ vs. t	$q_e = 1/\text{intercept}, K_2 = \text{slope}$

	Pseudo 1st			Type I Pseudo 2nd			Type II Pseudo 2nd		
	R^2	q_{cal}	K_1	R^2	q_{cal}	K_2	R^2	q_{cal}	K_2
PKM	0.0094	0.3887	0.0005	0.9966	21.5054	0.0044	0.9823	25.9740	0.0019
AC-PKM	0.4074	1.1220	0.0044	0.9961	72.9927	0.0008	0.9956	80.6452	0.0005
ACC	0.4750	1.5545	0.0039	0.9947	87.7193	0.0009	0.9830	98.0392	0.0005
	Type III Pseudo 2nd			Type IV Pseudo 2nd			Type V Pseudo 2nd		
	R^2	q_{cal}	K_1	R^2	q_{cal}	K_2	R^2	q_{cal}	K_2
PKM	0.9823	26.4738	0.0018	0.8447	24.5563	0.0023	0,4038	11,2867	0,0005
AC-PKM	0.9956	81.1957	0.0005	0.9348	79.6690	0.0005	0,3849	12,1359	0,0004
ACC	0.9830	99.5606	0.0005	0.8310	100.2432	0.0005	0,3582	33,3333	0,0001

in Gibbs free energy (ΔG) during the adsorption process could be calculated from its connection with thermodynamics based on Equation (5):

$$\Delta G^o = \Delta H^o - T\Delta S^o \quad (5)$$

where $G°$ is the change energy free standard (J/mol), $H°$ is the heat adsorption standard (J/mol), $S°$ is the change in entropy during adsorption (J/mol K) and T is the temperature (K). The Van't Hoff Equation (6) shows a relationship between the equilibrium constant and the free energy change.

$$\Delta G^o = -RT \ln K^o \quad (6)$$

Where R is an ideal gas constant of 8.314 (J/mol K) and K is an equilibrium constant. The equilibrium constant was calculated from the ratio of equilibrium adsorbate concentration still in solution, C_e (mg/L), to the quantity of adsorbate adsorbed per gram of adsorbent at equilibrium, q_e (mg/g). The following is how the equation for K is represented mathematically.

$$K = \frac{q_e}{C_e}° \quad (7)$$

In calculating the free energy change, equilibrium constant values were employed. The adsorption is usually confirmed to be spontaneous when the free energy change is negative. In order to derive the model parameters, Equation (5) was converted into a straight-line equation and plotted as $G°/T$ *vs.* $1/T$.

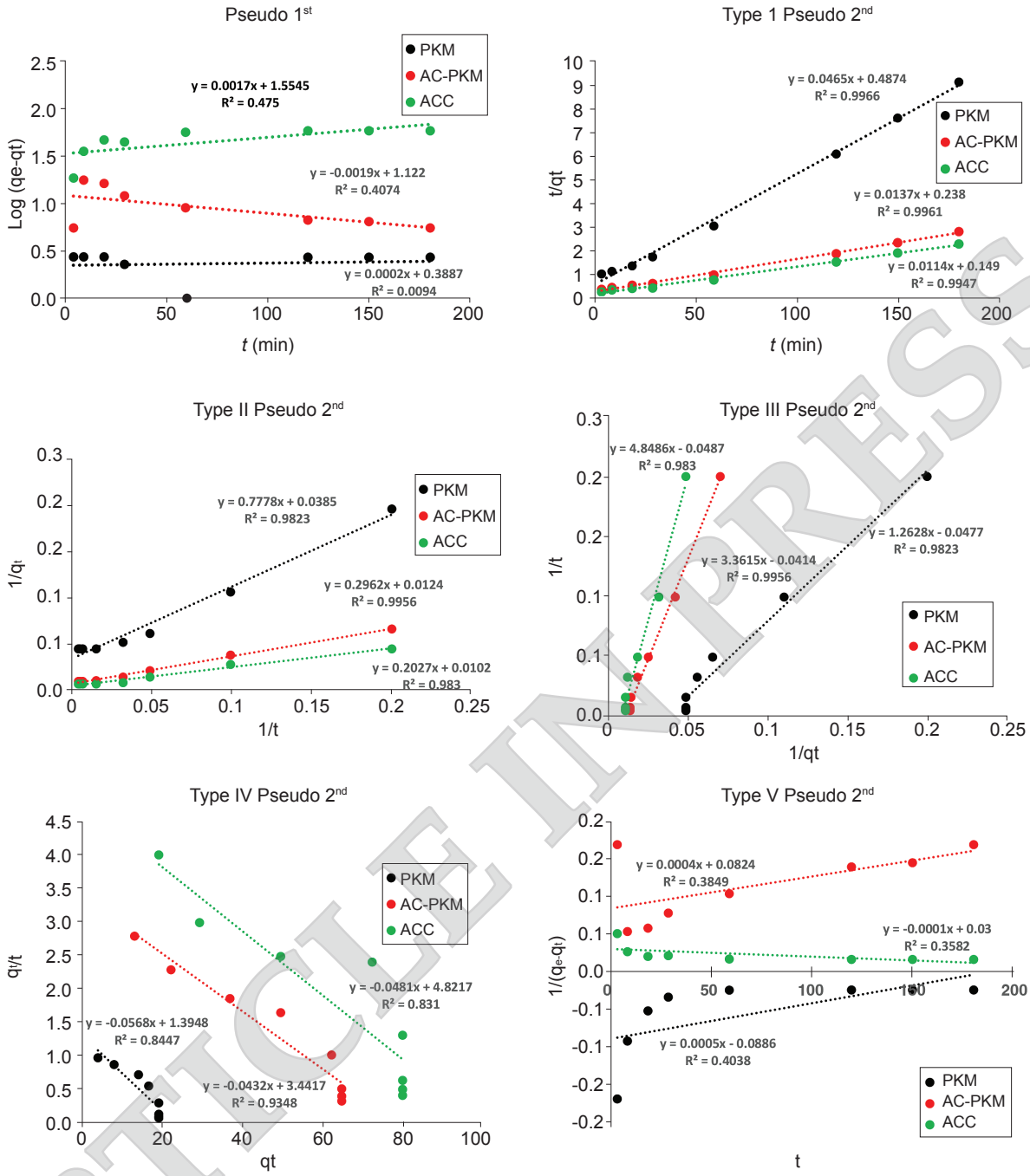

Figure 8. Pseudo-first-order and pseudo-second-order adsorption kinetics type I, II, III, IV, V plot of CFT removal on ACC, AC-PKM and PKM biomass.

Enthalpy and entropy values for adsorption were calculated using slope and intercept values. *Table 5* includes the information obtained for *G*, *H*, and *S*.

The change in free energy ($\Delta G°$), enthalpy ($\Delta H°$) and entropy ($\Delta S°$) were all predicted using thermodynamic analysis. The data for $G°$, $H°$, and $S°$ are shown in *Table 5* and *Figure 9*. The adsorption process is endothermic with a positive adsorption enthalpy value. On the other hand, the entropy was positive, associated with an increase in the system's randomness during adsorption. This thermodynamic parameter also shows that an increase in adsorption capacity will be obtained with an increase in temperature. However, it should be noted that at temperatures above 60°C (353 K), β-lactam antibiotics such as CFTs can degrade rapidly (Roca *et al.*, 2011).

CFT is an antibiotic widely used for surgical prophylaxis, pneumonia, respiratory infections and sepsis. The WHO (2014) recommended maximum daily dose of CFT is 2 g for adults (Anatomical Therapeutic Chemical/ATC J01DD04). Improper target use can increase the potential for CFT contamination in the waters. When the length of time the pollutant acts is examined, pollution

TABLE 5. THERMODYNAMIC MODEL FROM SAMPLE

Sample	Temperature (K)	ΔG (J/mol)	ΔH (J/mol)	ΔS (J/mol K)
PKM	298	289.73	8812.7	17 251
	303	268.30		
	313	176.65		
AC-PKM	298	-1 455.92	19 496.0	55 346
	303	-1 435.98		
	313	-1 344.59		
ACC	298	-2 071.71	25 768.0	78 193
	303	-1 763.25		
	313	-1 603.37		

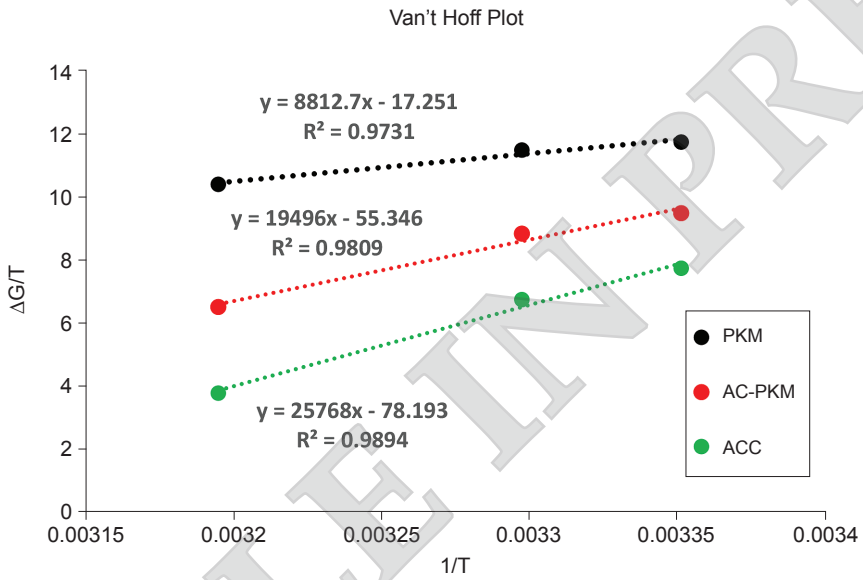

Figure 9. Van't Hoff Plot of CFT removal on ACC, AC-PKM and PKM biomass.

might be permanent, systematic, periodic, or accidental. The repercussions of water pollution have an impact on both the environment and human health (Gavrilescu, 2021). For this reason, reducing the risk of antibiotic residues from waste in hospitals is necessary. In this paper, adsorbent regeneration is not carried out because it is less economical and efficient. Thus, after adsorption, the adsorbent will be used as an alternative fuel. Further research is needed to investigate the release of carbon dioxides and other gases produced, thereby avoiding more harmful side pollutants.

Indonesia is the world's largest palm oil producer and produces PKM waste of 6 million tonnes per year. In addition, PKM waste is generally found in palm oil processing plants, making it easier to process it into activated carbon at a lower production price. Therefore, activated carbon based on PKM waste has great potential as an adsorbent that can be used as an alternative material in reducing antibiotic residues in water.

CONCLUSION

Modifying the glass wool-pyrolysis method at 750°C for 5 hr was developed to synthesize AC-PKM from palm kernel meal as an adsorbent for antibiotic residues. This method can maintain the surface-active functional groups on AC-PKM with a large specific surface area. The adsorption isotherm model for AC-PKM follows the Langmuir isotherm model at room temperature. The adsorption process is endothermic and spontaneous. Kinetics studies showed that CFT adsorption on AC-PKM followed a pseudo-second-order kinetic model. AC-PKM adsorbent can remove CFT levels greater than PKM, which is 26%. Although the percentage removal of AC-PKM is still lower than that of ACC. AC-PKM has potential in removing CFT and is an alternative treatment for reuse PKM biomass waste.

ACKNOWLEDGEMENT

This work was funded by PMDSU Scholarship, the Ministry of Educational and Culture of Republic Indonesia (Grant Number 4160/IT3.L1/PN/2020).

REFERENCES

Acelas, N; Lopera, S M; Porras, J and Torres-Palma, R A (2021). Evaluating the removal of the antibiotic cephalexin from aqueous solutions using an adsorbent obtained from palm oil fibre. *Molecules*, *26(11)*: 3340. DOI: 10.3390/molecules26113340.

Al-Riyami, I M; Ahmed, M; Al-Busaidi, A and Choudri, B S (2018). Antibiotics in wastewaters: A review with a focus on Oman. *Water Science App*., *8(7)*: 1-10. DOI: 10.1007/s132010180846-z.

Alekseev, V G (2010). Drug synthesis methods and manufacturing technology acid-base properties of penicillins and cephalosporins (a review). *Pharm. Chem. J., 44(1)*: 14-24.

Amiri, S; Sohrabi, M R and Motiee, F (2020). Optimization removal of the ceftriaxoxne drug from aqueous media with novel zero-valent iron supported on doped strontium hexaferrite nanoparticles by response surface methodology. *Anal. Chem., 5*: 5831-5840.

Ashtaputrey, S D and Ashtaputrey, P D (2016). Preparation and characterization of activated charcoal derived from orange peel. *J. Adv. Chem. Sci*., *2(3)*: 360-362.

Ayawei, N; Ebellegi, A N and Wankasi, D (2017). Modelling and interpretation of adsorption isotherms. *J. Chem., 2017*: 11. DOI: 10.1155/2017/3039817.

Ayele, A A; Gebresillassie, B M; Erku, D A; Gebreyohannes, E A; Demssie, D G; Mersha, A G and Tegegn, H G (2018). Prospective evaluation of ceftriaxone use in medical and emergency wards of Gondar University referral hospital, Ethiopia. *Pharmacol. Res. Perspect*., *6(1)*: 1-7. DOI: 10.1002/prp2.383.

Badi, Y M; Azari, A; Pasalari, H; Esrafili, A and Farzadkia, M (2018). Modification of activated carbon with magnetite Fe_3O_4 nanoparticle composite for removal of ceftriaxone from aquatic solutions. *J. Mol. Liq*., *261*: 146-154.

Bhandari, P S and Gogate, P R (2018). Kinetic and thermodynamic study of adsorptive removal of sodium dodecyl benzene sulfonate using adsorbent based on thermo-chemical activation of coconut shell. *J. Mol. Liq*., *252*: 495-505. DOI: 10.1016/j.molliq.2017.12.018.

Biasutti, M A; Anunziata, J D and Silber, J J (1992). N-π electron-donor-acceptor complexes-IV. The interaction of aliphatic amines with 1,3-dicyanobenzene in n-hexane. The importance of preferred orientation in the stability of the complexes. *Spectrochim. Acta Part A Mol. Spectrosc., 48(2)*: 169-173. DOI: 10.1016/0584-8539(92)80019-S.

Bozorginia, S; Jaafari, J; Taghavi, K; Ashraf, S D; Roohbakhsh, E and Naghipour, D (2021). Biosorption of ceftriaxone antibiotic by *Pseudomonas putida* from aqueous solutions. *Int. J. Environ. Anal. Chem*., *108*: 1-15. DOI: 10.1080/03067319.2021.18787858.

Browne, A J; Chipeta, M G; Haines-Woodhouse, G; Kumaran, E P A; Hamadani, B H K; Zaraa, S; Henry, N J; Deshpande, A; Reiner, R C; Day, N P J; Lopez, A D; Dunachie, S; Moore, CE; Stergachis, A; Hay, S I and Dolecek, C (2021). Global antibiotic consumption and usage in humans, 2000-18: A spatial modelling study. *Lancet Planet. Health*., *5(12)*: e893-e904. DOI: 10.1016/S2542-5196(21)00280-1.

Cassol, O G; Gallon, R; Schwaab, M; Barbosa-Coutinho, E; Júnior, J B and Pinto, J C (2014). Statistical evaluation of non-linear parameter estimation procedures for adsorption equilibrium models. *Adsorp. Sci. Technol., 32(4)*: 257-273.

De Diego, M; Godoy, G and Mennickent, S (2010). Chemical stability of ceftriaxone by a validated stability-indicating liquid chromatographic method. *J. Chil. Chem. Soc*., *55(3)*: 335-337. DOI:10.4067/S0717-97072010000300013.

De Gisi, S; Lofrano, G; Grassi, M and Notarnicola, M (2016). Characteristics and adsorption capacities of low-cost sorbents for wastewater treatment: A review. *Sustain. Mater. Technol*., *9*: 10-40. DOI: 10.1016/j.susmat.2016.06.02.

Fahmi, A G; Abidin, Z; Kusmana, C; Kharisma, D; Prajaputra, V and Rahmawati, W R (2019). Preparation and characterization of activated carbon from palm kernel shell at low temperature as an adsorbent for methylene blue. *IOP Conference Series: Earth and Environmental Science. 399 pp*.

Fahmi, A G; Abidin, Z; Kusmana, C and Noor, E (2022). Versatile synthesis of activated carbon from coconut shells: A method for cyanide adsorption in artisanal and small-scale gold mining wastewater. *J. Degrade. Min. Land Manage., 9(4)*: 3685-3693.

Feng, P; Li, J; Wang, H and Xu, Z (2020). Biomass-based activated carbon and activators: Preparation of activated carbon from corncob by chemical activation with biomass pyrolysis liquids. *ACS Omega*., *5(37)*: 24064-24072. DOI: 10.1021/acsomega.0c03494.

Gavrilescu, M (2021). Water, soil, and plants interactions in a threatened environment. *Water*, *13*: 2746. DOI: 10.3390/w13192746.

Gonzalez, D; Golab, J T; Eilert, J Y; Wang, R and Kaduk, J A (2020). Crystal structure of ceftriaxone sodium hemiheptahydrate, $C18H16N8O7S3Na_2(H_2O)3.5$. *Powder Differ., 35(3)*: 206-212. DOI: 10.1017/S0885715620000299.

Gumus, R H; and Okpeku, I (2015). Production of activated carbon and characterization from snail shell waste. *Adv. Chem. Eng. Sci.*, *05(01)*: 51-61. DOI: 10.4236/aces.2015.51006.

Hassan, M; Zhu, G; Lu, Y Z; Al-Falahi, A H; Lu, Y; Huang, S and Wan, Z (2021). Removal of antibiotics from wastewater and their problematic effects on microbial communities by bioelectrochemical technology: Current knowledge and future perspectives. *Environ. Eng. Res., 26(1)*: 1-15. DOI: 10.4491/eer.2019.405.

Hu Z; and Gao Z (2018). High-surface-area activated red mud for efficient removal of methyleneblue from wastewater. *Adsorpt. Sci. Technol*., *36(1-2)*: 62-79. DOI: 10.1177/0263617416684348.

de Ilurdoz, M S; Sadhwani, J J; and Reboso, J V (2022). Antibiotic removal processes from water and wastewater for the protection of the aquatic environment - A review. *J. Water Process. Eng*., *45*: 102474. DOI: 10.1016/j.jwpe.2021.102474.

Jasper, E E; Ajibola, V O and· Onwuka, J C (2020). Nonlinear regression analysis of the sorption of crystal violet and methylene blue from aqueous solutions onto an agro-waste derived activated carbon. *Appl. Water Sci., 10*: 132. DOI: 10.1007/s13201-020-01218-y.

Karri, R R; Sahu, J N; and Jayakumar, N S (2017). Optimal isotherm parameters for phenol adsorption from aqueous solutions onto coconut shell based activated carbon: Error analysis of linear and non-linear methods. *J. Taiwan Inst. Chem. Eng., 80*: 472-487. DOI: 10.1016/j.jtice.2017.08.004.

Khan, M Y; Roy, M; Rawal, R K and Bansal, U K (2017). Ceftriaxone for life. *Asian J. Pharm. Res., 7(1)*: 35-48. DOI: 10.5958/2231-5691.2017.00007.

Kharrazi, S M; Soleimani, M; Jokar, M; Richards, T; Pettersson, A and Mirghaffari, N (2021). Pretreatment of lignocellulosic waste as a precursor for synthesis of high porous activated carbon and its application for Pb (II) and Cr (VI) adsorption from aqueous solutions. *Int. J. Biol. Macromol., 180*: 299-310. DOI: 10.1016/j.ijbiomac.2021.03.078.

Kordestani, B; Takdastan, A; Jalilzadeh Yengejeh, R and Neisi, A K (2020). Photo-Fenton oxidative of pharmaceutical wastewater containing meropenem and ceftriaxone antibiotics: Influential factors, feasibility, and biodegradability studies. *Toxin. Rev., 39(3)*: 292-302. DOI: 10.1080/15569543.2018.1520261.

Mahmoud, M E; El-Ghanam, A M; Mohamed, R H A and Saad, S R (2020). Enhanced adsorption of levofloxacin and ceftriaxone antibiotics from water by assembled composite of nanotitanium oxide/chitosan/nano-bentonite. *Mater. Sci. Eng., 108(2019)*: 110199. DOI: 10.1016/j.msec.2019.110199.

Maulina, S; Handika, G; Irvan and Iswanto, A H (2020). Quality comparison of activated carbon produced from oil palm fronds by chemical activation using sodium carbonate versus sodium chloride. *J. Korean Wood Sci. Technol*., *48(4)*: 503-512. DOI: 10.5658/WOOD.2020.48.4.503.

Mensah, K B and Ansah, C (2016). Irrational use of antibiotics and the risk of diabetes melitus in Ghana. *Ghana Med. J., 50(2)*: 107-114. DOI: 10.4314/gmj.v50i2.9.

Okeola, O F; Odebunmi, E O and Ameen, O M (2012). Comparison of sorption capacity and surface area of activated carbon prepared from *Jatropha curcas* fruit pericarp and seed coat. *Bull. Chem. Soc. Ethiopia*., *26(2)*: 171-180. DOI: 10.4314/bcse.v26i2.2.

Olesen, S W; Barnett, M L; Macfadden, D R; Brownstein, J S; Hernández-Díaz, S; Lipsitch, M and Grad, Y H (2018). The distribution of antibiotic use and its association with antibiotic resistance. *Elife*, *7*: 1-15. DOI: 10.7554/eLife.39435.

Osman, N B; Shamsuddin, N and Uemura, Y (2016). Activated carbon of oil palm empty fruit bunch (EFB); Core and shaggy. *Procedia Eng*., *148*: 758-764. DOI: 10.1016/j.proeng.2016.06.610.

Prajwal, S; Vasudevan, V N; Sathu, T; Irshad, A and Pame, K (2017). Antibiotic residues in food animals: Causes and health effects. *Pharma. Innov. J., 6(12)*: 01-04.

Rivas, B L; Oñate, P and Palacio, D A (2020). Removal of oxytetracycline by polimers: An overview. *J. Chil. Chem. Soc*., *4*: 4943-4947.

Roca, M; Villegas, L; Kortabitarte, M L; Althaus, R L and Molina, M P (2011). Effect of heat treatments on stability of β-lactams in milk. *J. Dairy Sci*., *94*: 1155-1164. DOI: 10.3168/jds.2010-3599.

Rugayah, A F; Astimar, A A and Norzita, N (2014). Preparation and characterisation of activated carbon from palm kernel shell by physical activation with steam. *J. Oil Palm Res*., *26(3)*: 251-264.

Saied, M El; Shaban, S A; Mostafa, M S; and Naga, A O A (2022). Efficient adsorption of acetaminophen from the aqueous phase using low-cost and renewable adsorbent derived from orange peels. *Biomass Convers. Biorefin., March 2022*. 18 pp. DOI: 10.1007/s13399-022-02541-x.

Santhiarsa, I G N N (2021). Effect of variations in pyrolysis reactor with glass wool equipped and without glass wool on the weight of the oil produced. *J. Mech. Eng. Sci. Technol*., *5(2)*: 89-95.

Schultz, J; Capobianco, G; da Silva Veiga, P A; Fornari, M R; Antonangelo, A R; Tebcherani, S M; Mangrich, A S and Pianaro, S A (2020). Sustainable activated carbon obtained as a by-product of the sugar and alcohol industry for removal of amoxicillin from aqueous solution. *Energy, Ecol. Environ*., *5(6)*: 433-443. DOI:10.1007/s40974-020-00173-3.

Sharma, G; Kaur, M; Punj, S and Singh, K (2020). Biomass as a sustainable resource for value-added modern materials: A review. *Biofuels, Bioprod. Biorefin*., *14(3)*: 673-695. DOI: 10.1002/bbb.2079.

Shi, X; Karachi, A; Hosseini, M; Yazd, M S; Kamyab, H; Ebrahimi, M and Parsaee, Z (2020). Ultrasound wave assisted removal of Ceftriaxone sodium in aqueous media with novel nanocomposite g-C3N4/MWCNT/Bi2WO6 based on CCD-RSM model. *Ultrason. Sonochem., 68*: 104460. DOI: 10.1016/j.ultsonch.2019.01.018.

Shipingana, L N N; Shivaraju, H P and Yashas, S R (2022). Quantitative assessment of pharmaceutical drugs in a municipal wastewater and overview of associated risks. *Appl. Water Sci., 12(16)*: 1-9.

Song, Y; Sackey, E A; Wang, H and Wang, H (2019). Adsorption of oxytetracycline on kaolinite. *PLOS One*., *14(11)*: 1-13. DOI: 10.1371/journal.pone.0225335.

Tani, D; Setiaji, B; Trisunaryanti, W and Syoufian, A (2014). Effect of activation time on chemical structure and quality of coconut shell activated carbon. *Asian J. Sci. Technol*., *5(9)*: 553-556.

Ukanwa, K S; Patchigolla, K; Sakrabani, R and Anthony, E (2020). Preparation and characterization of activated carbon from palm mixed waste treated with trona ore. *Molecules, 25(21)*: 1-18. DOI: 10.3390/molecules25215028.

Vafakhah, S; Bahrololoom, M E and Saeedikhani, M (2016). Adsorption kinetics of cupric ions on mixture of modified corn stalk and modified tomato waste. *J. Water Resource Prot*., *8*: 1238-1250.

WHO (2014). Safe management of wastes from healthcare activities.

Widayati, A; Suryawati, S; De Crespigny, C and Hiller, J E (2011). Self medication with antibiotics in Yogyakarta City Indonesia: A cross sectional population-based survey. *BMC Res Notes, 4(1)*: 491. DOI: 10.1186/1756-0500-4-491.

Wu, Z; Ye, X; Liu, H; Zhang, H; Liu, Z; Guo, M; Li, Q and Li, J (2020). Interactions between adsorbents and adsorbates in aqueous solutions. *Pure Appl. Chem*., *92(10)*: 1655-1662. DOI: 10.1515/pac-2019-1110.

Xiao, F; Bedane, A H; Zhao, J X; Mann, M D and Pignatello, J J (2018). Thermal air oxidation changes surface and adsorptive properties of black carbon (char/biochar). *Sci. Total Environ., 618*: 276-283. DOI: 10.1016/j.scitotenv.2017.11.008.

Yu, J; Kang, Y; Yin, W; Fan, J and Guo, Z (2020). Removal of antibiotics from aqueous solutions by a carbon adsorbent derived from protein-waste-doped biomass. *ACS Omega*, *5(30)*: 19187-19193. DOI: 10.1021/acsomega.0c02568.

Zango, Z U; Jumbri, K; Sambudi, N S; Ramli, A; Bakar, N H H A; Saad, B; Rozaini, M N H; Isiyaka, H A; Jagaba, A H; Aldaghri, O and Sulieman, A (2020). A critical review on metal-organic frameworks and their composites as advanced materials for adsorption and photocatalytic degradation of emerging organic pollutants from wastewater. *Polymers (Basel)*., *12(11)*: 1-42. DOI: 10.3390/polym12112648.

Zhao, Y; Liang, X; Wang, Y; Shi, H; Liu, E; Fan, J and Hu, X (2018). Degradation and removal of ceftriaxone sodium in aquatic environment with Bi2WO6/g-C3N4 photocatalyst. *J. Colloid Interface Sci., 523*: 7-17. DOI: 10.1016/j.jcis.2018.03.078.